

All-Printed Electroencephalography Array for In Vivo Neural Recordings


Eleonora Borda, Laura Ferlauto, Jürg Schleuniger, Alessandro Mustaccio, Fabian Lütolf, Arnold Lücke, Sören Fricke, Nenad Marjanović, and Diego Ghezzi*

Bioelectronic and neuroprosthetic interfaces rely on implanted microelectrode arrays (MEAs) to interact with the human body. Printing techniques, such as inkjet and screen printing, are attractive methods for the manufacturing of MEAs because they allow flexible, room-temperature, scalable, and cost-effective fabrication processes. Herein, the fabrication of all-printed electroencephalography arrays made by inkjet printing of platinum and screen printing of polyimide is shown. Next, mechanical and electrochemical characterizations are performed. As a proof of concept, in vivo visually evoked cortical potentials are recorded in rabbits upon flash stimulation. Lastly, it is shown that the all-printed electroencephalography arrays are not cytotoxic. Altogether, the results enable the use of printed MEAs for neurological applications.

Microelectrode array (MEA) devices are essential to interface with electroactive tissues, such as the nervous system and muscles.^[1] Several biomedical devices rely on macro- and micro-electrodes to deliver electrical stimuli or to record electrical activity to and from the tissue, such as cardiac pacemakers, deep brain stimulators, cochlear implants, retinal prostheses, and electroencephalography arrays.^[2–6] Medical-grade MEAs are mostly hand-made by skilled technicians, whereas only a few rely on clean-room processes derived from the silicon industry.^[7] Although clean-room processes have high resolution and reproducibility, they constrain the fabrication of medical-grade MEAs mostly because of high production cost and chemical or thermal incompatibility with flexible or elastic substrates. In addition, clean-room processes limit the size of MEAs to the wafer dimension and the number of possible layouts due to expensive lithographic masks. Printing methods can overcome the issues mentioned previously because they are based on low-temperature, flexible, cost-effective, and large area processes.

E. Borda, Dr. L. Ferlauto, Prof. D. Ghezzi
 Medtronic Chair in Neuroengineering
 Center for Neuroprosthetics and Institute of Bioengineering
 School of Engineering
 École Polytechnique Fédérale de Lausanne
 Chemin des Mines 9, 1202 Geneva, Switzerland
 E-mail: diego.ghezzi@epfl.ch

J. Schleuniger, A. Mustaccio, Dr. F. Lütolf, A. Lücke, Dr. S. Fricke,
 Dr. N. Marjanović
 CSEM Muttenz
 Tramstrasse 99, 4132 Muttenz, Switzerland

 The ORCID identification number(s) for the author(s) of this article can be found under <https://doi.org/10.1002/adem.201901403>.

DOI: 10.1002/adem.201901403

Platinum is the material of choice for both recording and stimulation electrodes in most of the medical-grade MEAs because of its mechanical and chemical stability, ease of processing from foils, and its good electrochemical performance.^[8,9] In addition, the faradaic reactions are confined to a surface monolayer, therefore often called pseudocapacitive, which is an appealing feature for safe electrical stimulation.^[10] Despite the relevance of platinum in the medical field, printed platinum-based MEAs were not yet investigated. In this article, we report the fabrication, characterization, and validation of a fully-printed, flexible,

platinum-based electroencephalography array.

Platinum-based electroencephalography arrays (Figure 1a,b) were printed using a commercial platinum precursor ink (16512, Ceimig Limited) on 60 μm thick polyimide foils (PI; Kapton HN, DuPont). Each electroencephalography array consisted of 16 (2×8) square electrodes of 450 μm in size with a center-to-center pitch of 1120 μm (Figure 1a). Electrodes, tracks, and pads were printed with a single scan resulting in a line thickness of 130.8 ± 39.3 nm (mean \pm standard deviation [SD], $n = 18$ lines from $N = 3$ arrays; Figure 1c), whereas the line width was 246 ± 12.8 μm (mean \pm SD, $n = 9$ lines from $N = 3$ arrays). After printing and precuring (200 $^{\circ}\text{C}$, 20 min), the line resistance, measured from electrode to pad, was 1.26 ± 0.19 k Ω (mean \pm SD, $n = 6$ lines from $N = 1$ array). Such a high resistance would have hampered the capability of the array to detect neuronal activity. Photonic sintering (PS) was performed to reduce the line resistance by a factor of 2.5, lowering it to 515.7 ± 28.4 Ω (mean \pm SD, $n = 16$ lines from $N = 1$ array; Figure 1d, column “After PS”). Afterward, the arrays were encapsulated with a layer of screen-printed PI precursor (HP-1000G2, Hitachi Chemical) having a thickness of 4.37 ± 0.93 μm (mean \pm SD, $n = 9$ measures from $N = 2$ arrays). To expose the electrodes and pads, circular openings were designed in the encapsulation layer with 300 and 550 μm nominal diameters, respectively (Figure 1b). The measured apertures were 300.2 ± 23.5 μm for the electrodes and 534.1 ± 18.7 μm for the pads (mean \pm SD, $n = 48$ measures from $N = 3$ arrays). After encapsulation, the line resistance was slightly reduced to 495.3 ± 27.1 Ω (mean \pm SD, $n = 16$ lines from $N = 1$ array; Figure 1d, column “After PI”; $p < 0.0001$, two-tailed paired t -test). This reduction might be associated with the additional thermal treatment performed after screen printing. Overall,

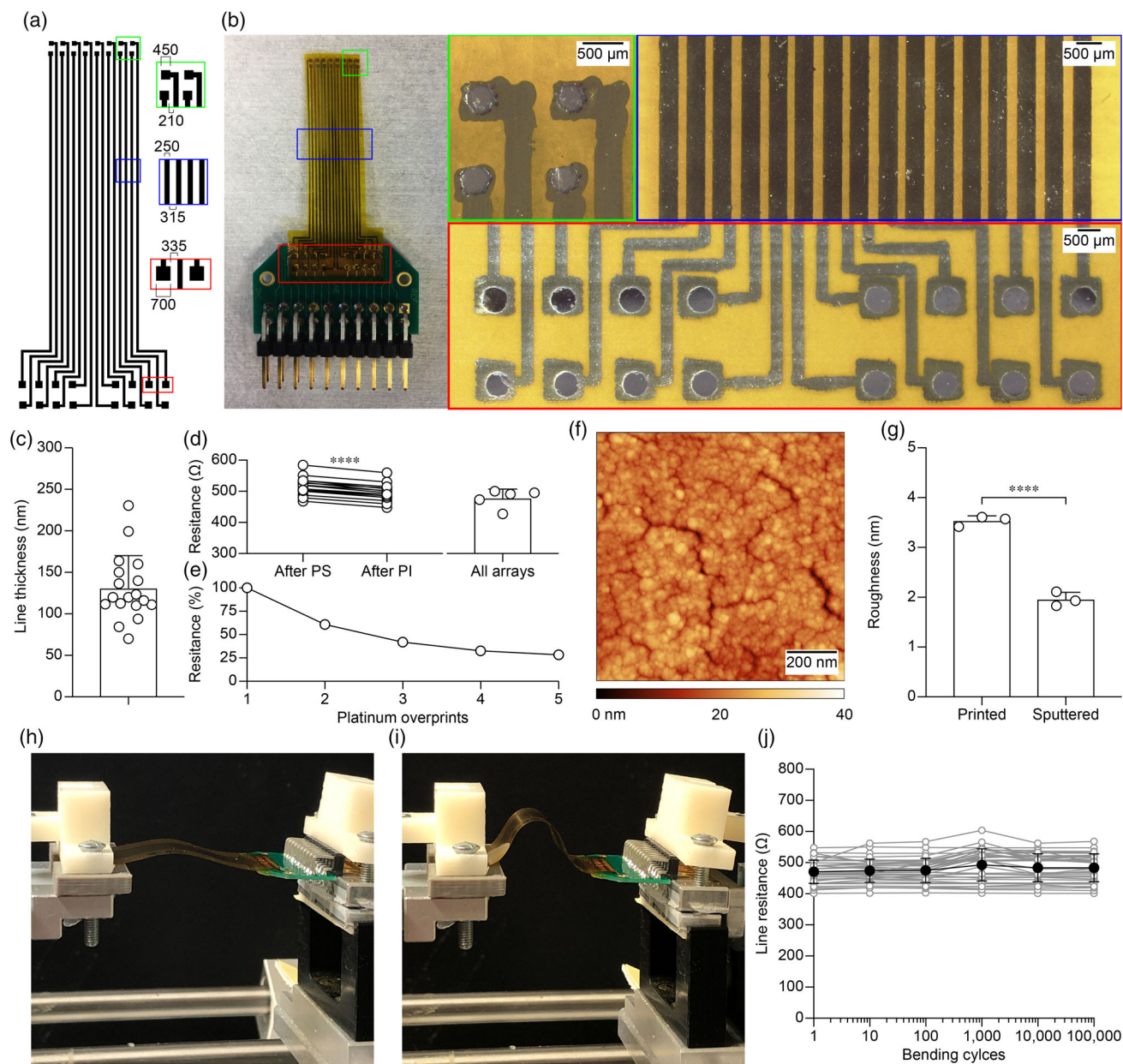


Figure 1. Printed platinum-based electrocorticography electrode array. a) Printing layout. The insets show the electrodes (green), tracks (blue), and pads (red). The quotes are reported in micrometers. b) Picture of an assembled array connected to a printed circuit board. The green, blue, and red boxes show a magnified view of the electrodes (green), tracks (blue), and pads (red). c) Mean (\pm SD) line thickness measured across $n = 18$ lines from $N = 3$ arrays. d) Line resistance from pad to electrode. Left: comparison of the resistance values after PS and after PI encapsulation ($n = 16$ electrodes from $N = 1$ array). Right: mean (\pm SD) line resistance values across $N = 5$ arrays. For each array, the values of $n = 16$ electrodes were averaged together. e) Normalized line resistance with multiple overprints of platinum. f) Example of an atomic force microscopy image ($1 \mu\text{m} \times 1 \mu\text{m}$) of a printed platinum electrode. g) Mean (\pm SD) roughness values for printed ($3.533 \pm 0.100 \text{ nm}$) and sputtered platinum ($1.957 \pm 0.142 \text{ nm}$) electrodes obtained from the corresponding images ($n = 3$ electrodes from $N = 1$ array for each condition). Printed platinum-based electrocorticography electrode array during a bending test in the h) initial position and i) final position. j, k) The bending radius was 9.1 mm , and the bending speed was 10 mm s^{-1} . l) Line resistance variation as a function of multiple bending cycles. The gray dots and lines are individual electrodes ($n = 35$ electrodes from $N = 3$ array), whereas the black dots and line are the mean \pm SD.

the average line resistance of the printed electrodes was $477.3 \pm 29.9 \Omega$ (mean \pm SD; $n = 16$ electrodes, $N = 5$ arrays; Figure 1d, column "All arrays"). Moreover, the line resistance can be further decreased by printing multiple layers of platinum

(Figure 1e): this is an established technique that was already shown for feedlines printed in gold.^[11] For printed platinum, the line resistance was also reduced coherently with the number of multiple overprints. Indeed, a considerable reduction was

observed up to three overprints (42.00% of the initial value with three overprints), whereas a minor decrease was reported with more overprints (28.35% of the initial value with five overprints).

Next, the surface roughness of the printed platinum electrodes was measured (Figure 1f), which resulted significantly higher than the one of sputtered platinum electrodes ($p < 0.0001$, two-tailed unpaired t -test; $n = 3$ electrodes each; Figure 1g). This higher surface roughness is a desirable feature for microelectrodes because it should provide better electrochemical performance, due to the increase of the electrochemical surface area.

The choice of PI as substrate material relied mainly on its flexibility, a crucial feature when designing medical MEAs to interface soft tissues such as the brain. Thus, we also tested the mechanical robustness of the printed arrays upon cyclic bending. Printed platinum-based electrocorticography arrays were stable upon 100 000 cycles of flexions (bending radius: 9.1 mm; speed: 10 mm s⁻¹; Figure 1h,i). The line resistance was monitored over cycles, and there was no statistically significant change after each bending cycle ($p = 0.2820$, one-way ANOVA; Figure 1l).

To characterize in vitro the performance of printed platinum-based electrodes in an aqueous environment, we performed electrochemical impedance spectroscopy (EIS) and cyclic voltammetry (CV; Figure 2). The impedance magnitude (Figure 2a),

the impedance phase (Figure 2b), and the CV curves (Figure 2c) of printed platinum electrodes (black lines, $n = 15$ electrodes from $N = 1$ array) showed a shape qualitatively similar to the one of sputtered electrodes of equivalent surface area (gray line, average of $n = 16$ electrodes from $N = 1$ array). However, the impedance magnitude (Figure 2a,d) and the impedance phase (Figure 2b,e) were significantly lower ($p < 0.0001$, unpaired t -test), whereas the charge-storage capacity (CSC) was significantly higher ($p < 0.0001$, Mann-Whitney test; Figure 2c,f), likely due to the higher roughness of the printed platinum. In MEAs, a higher CSC and a lower impedance magnitude correlate with improved performance during tissue stimulation and recording.^[10] The values of the impedance magnitude and phase were taken at 1 kHz, which is reference frequency in neurotechnology. EIS and CV were measured for five printed arrays (Figure 2d-f, columns "All arrays"). The results showed that the impedance magnitude, the impedance phase, and the CSC are reproducible not only within the same array but also between arrays (mean \pm SD, for each of the $N = 5$ arrays, the data from all the $n = 15$ electrodes were averaged). For printed arrays, only 15 electrodes out of 16 were working during electrochemical experiments. Because the line conductivity was verified for all of the electrodes, this might be associated to the manual bonding procedure of the array to a printed circuit

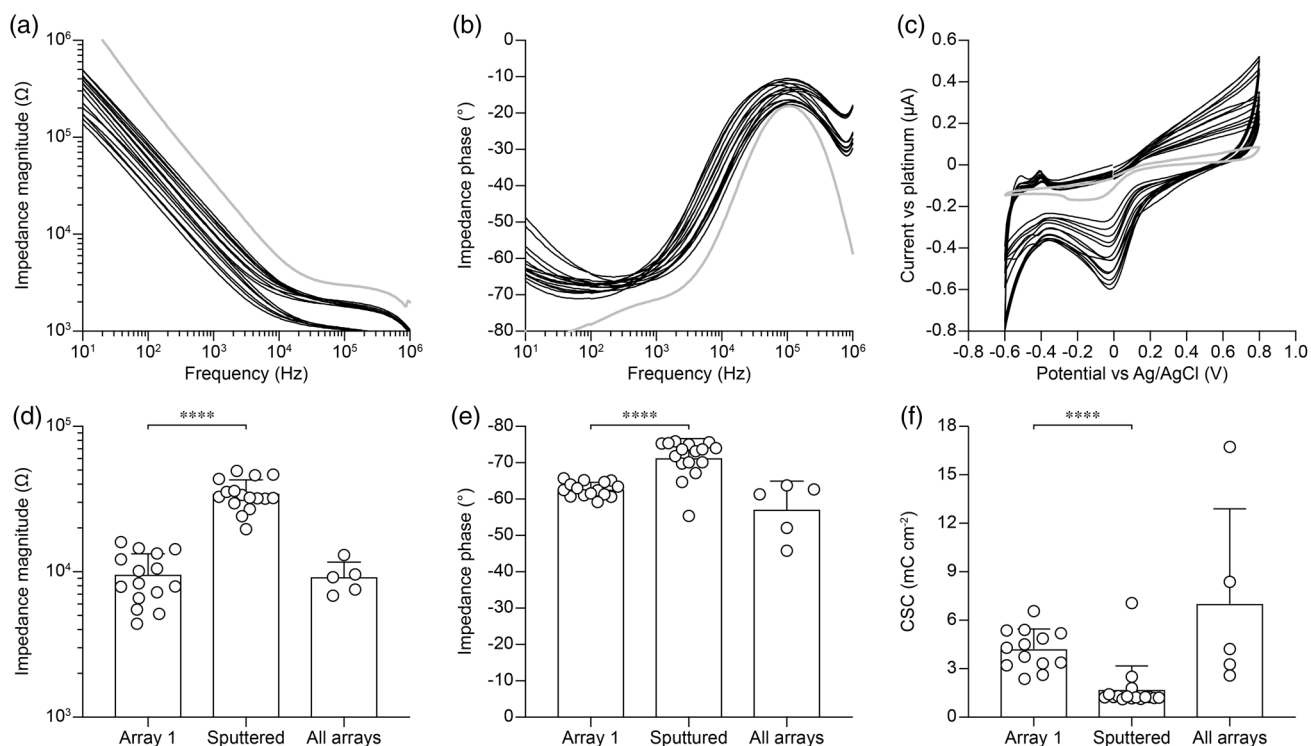


Figure 2. Electrochemical characterization of electrocorticography electrode arrays with printed platinum. a) Impedance magnitude, b) impedance phase, and c) CV measured on a printed array (black lines, $n = 15$ electrodes from $N = 1$ array). The gray line is the average from sputtered platinum electrodes of equivalent surface area (300 μm diameter, average of $n = 16$ electrodes from $N = 1$ array). Quantification (mean \pm SD) of d) impedance magnitude at 1 kHz, e) impedance phase at 1 kHz, and f) charge storage capacity for the $n = 15$ printed electrodes (columns "Array 1"), the $n = 16$ sputtered electrodes (columns "Sputtered"), and all the printed array (columns "All arrays"; for each array, the values of the $n = 16$ electrodes were averaged together). Impedance magnitude: $9599 \pm 3734 \Omega$ ("Array 1"), $34\,531 \pm 8284 \Omega$ ("Sputtered"), $9248 \pm 2409 \Omega$ ("All arrays"); impedance phase: $-62.70 \pm 1.960^\circ$ ("Array 1"), $-71.31 \pm 5.336^\circ$ ("Sputtered"), $-57.13 \pm 7.835^\circ$ ("All arrays"); CSC: $4.222 \pm 1.237 \text{ mC cm}^{-2}$ ("Array 1"), $1.713 \pm 1.467 \text{ mC cm}^{-2}$ ("Sputtered"), $7.034 \pm 5.869 \text{ mC cm}^{-2}$ ("All arrays").

board used to connect the array to the measuring instrumentation (Figure 1b).

Next, we provided proof-of-concept evidence about the use of printed platinum-based electrocorticography arrays in vivo to detect sensory-evoked cortical activity. The printed array was placed onto the visual cortex of an anesthetized rabbit (Figure 3a), and visually evoked potentials were recorded upon flash stimulation of the eye contralateral to the recording hemisphere (Figure 3b). Recordings showed the appearance of the classical peaks of the visually evoked potentials (Figure 3c) with an amplitude modulated by the stimulus luminance (Figure 3d). In addition, the biocompatibility of the printed arrays was also proven. According to ISO 10993-5: Biological Evaluation of Medical Devices, in vitro cytotoxicity was evaluated via an extraction test on the murine fibroblastic L929 cells.^[12] Cell viability was estimated via an XTT assay on triplicate culture wells for each sample. Results on the printed platinum-based electrocorticography arrays showed no cytotoxic effect (sample 1: 100% viability; sample 2: 92.4% viability), whereas positive control has 0.17% viability and negative control has 100% viability (all numbers are averages of three repetitions). Therefore, no cytotoxic effect is demonstrated for viability above 70% compared with the negative control.

The main goal of this study was to demonstrate that printed flexible platinum-based electrocorticography arrays can be used in neurophysiological investigations. To do so, the printed geometrical features were kept similar to the ones of conventional electrocorticography arrays. However, the minimal resolution that could be achieved with this combination of ink, substrate, and equipment was further investigated (Figure 4).

A minimum single-dot size of about 200 μm with a minimum dot separation of 20 μm was obtained (without in-flight dispensing mode; Figure 4a). For lines, a minimum line width of 220 μm with a line spacing of 50 μm was obtained (with in-flight dispensing mode; Figure 4b). Lastly, excellent line stability was also observed for multiple overprints (Figure 4c).

Printing technology possesses several advantages compared with clean-room microfabrication techniques, such as low-temperature, flexible, cost-effective, and large-area processes. These aspects might be relevant for the production of medical-grade MEAs, currently mostly hand-made. In this work, exclusively commercially available materials were used, which is an advantage for a faster clinical translation of these electrocorticography arrays.

Printed MEAs were already tested to detect the pressure ulcer in rats and pulse rate and arterial blood oxygenation in humans, but the use of printing techniques for functional materials in biomedical implants is still uncommon.^[13–15] Concerning MEAs for sensing and stimulating electrogenic tissue, other groups already reported the fabrication of inkjet-printed electrodes for in vitro applications. Inkjet-printed gold MEAs were used in vitro to detect action potentials from cardiomyocyte-like HL-1 cells cultured on top of the device.^[11] Uncoated gold is usually a candidate for recording electrodes. However, platinum is a common choice for both recording and stimulating electrodes.^[9] Therefore, a printed platinum-based array has the advantage to be more versatile in neurophysiological investigations. Among other materials, inkjet-printed silver/poly(3,4-ethylenedioxythiophene)-poly(styrenesulfonate) were proposed for neuromuscular cartography.^[16]

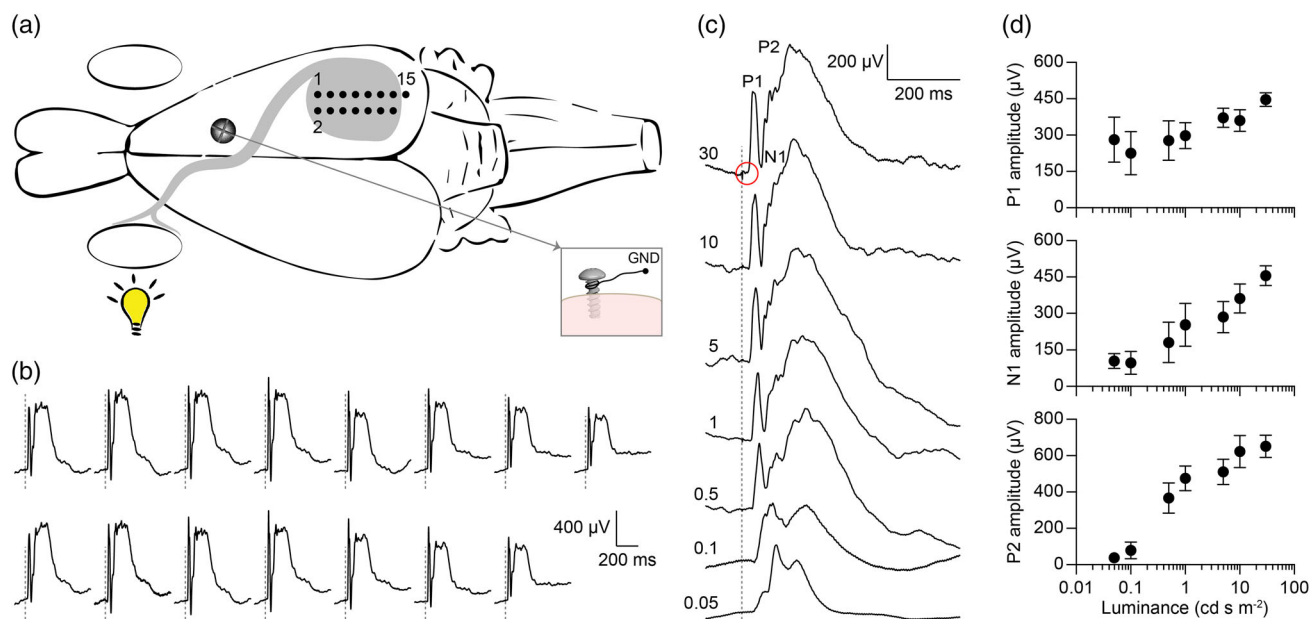


Figure 3. Validation in vivo. a) Recordings of visually evoked cortical potentials were performed with the printed electrocorticography array covering the visual cortex and a flash stimulation (4 ms, Ganzfeld white LED) in the contralateral eye. b) Example of responses (synchronous average of ten repetitions) to a flash illumination of 30 cd s^{-2} . The dashed gray lines show the occurrence of the flash. c) Example traces obtained from one recording channel at increasing flash luminance values. The main peaks (P1, N1, and P2) are visible. The dashed line shows the occurrence of the flash. The red circle shows the stimulation artifact. d) Quantification of the peak amplitudes as a function of the flash luminance. Each data point is the mean ($\pm\text{SD}$) of the 15 recording electrodes. For each electrode, ten consecutive recordings were averaged.

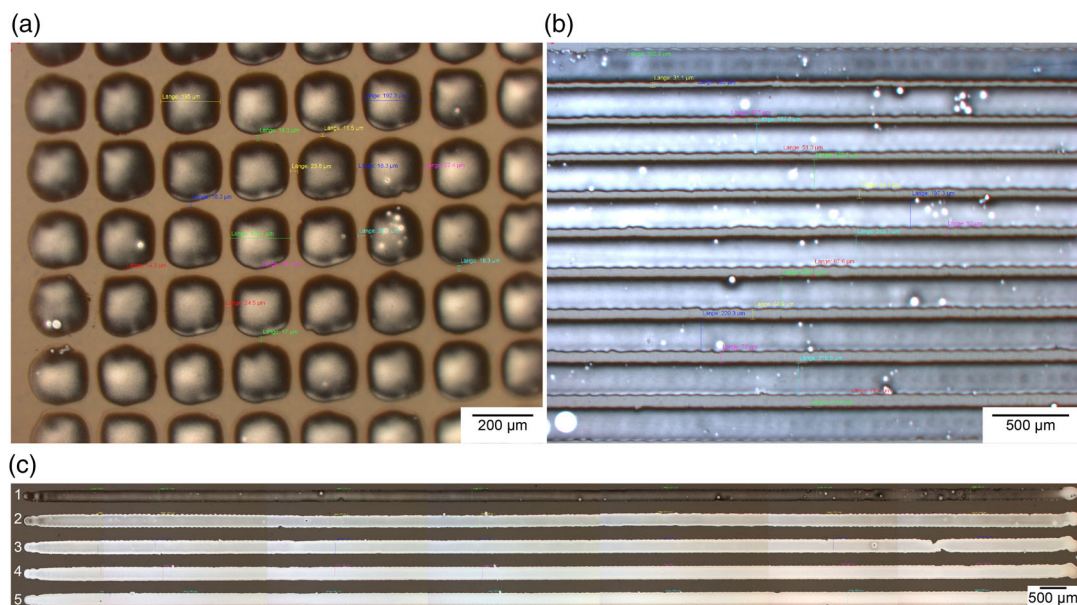


Figure 4. Printing resolution. a) An array of printed single dots. b) An array of printed single lines. c) Multiple overprints of 2 cm-long platinum lines. The number of overprints is shown on the left.

To our knowledge, this is the first time that printed flexible platinum-based electrocorticography arrays are used in neurophysiological investigations *in vivo*. Further studies will be required to grant the use of printed arrays to monitor or treat neurological disease in humans. Nonetheless, our results represent the first step in this direction.

Experimental Section

Electrode Array Printing: Printing was performed on polyimide foils (μm -thick Kapton HN, DuPont) previously rinsed with isopropyl alcohol. An organometallic nonparticulated platinum precursor with 12 wt% platinum metal content was used (16512, Ceimig Limited). The ink was stored at 4 °C. Before use, the ink was filtrated with a polytetrafluoroethylene filter with 0.45 μm pore size. A single-nozzle inkjet printer (Microdrop Technologies GmbH; Germany) with a 50 μm glass capillary (MDK-140) was used for printing. The printer vacuum chuck was kept at 85 °C, which caused the print head to gradually heat up from room temperature to 40 °C during the printing process. The original layout was discretized to fit a drop spacing of 0.06 mm. Printing was performed with in-flight dispensing mode (20 mm s⁻¹). After printing, the device was precured in a reflow oven at 200 °C for 20 min.

PS: PS was performed with a Pulse Forge 1300 (NovaCentrix, TX, USA). Three 700 μs pulses were delivered with an interval of 1 ms. The bank voltage was 440 V, corresponding to light energy of 5476 mJ cm⁻². During light exposure, the samples were cooled by airflow. The simulation software tool correlates a light pulse into a sintering temperature of \approx 1300 °C.

Screen Printing: Screen printing was performed with an Aurel VS1520 printer, with the following parameters: print speed 125 mm s⁻¹, print type 2 directions print, print gap 2 mm, pressure 10 kg, and squeegee 45°. Meshes were manufactured by Koenen GmbH. After printing, the screen-printed layers were heated on a hot plate at 100 °C for 10 min and then cured in reflow oven at 250 °C for 5 min.

Electrode Arrays with Sputtered Platinum: Arrays were fabricated as previously described.^[17] Briefly, sputtered MEAs were fabricated on 4 in. silicon wafers (thickness 525 μm) with a titanium–tungsten alloy/aluminum release layer (TiW/Al, 200 nm/1 μm). A PI layer (HD MicroSystems

PI2611, 10 μm) was spin-coated (1400 rpm for 40 s) and then cured by a soft bake (5 min at 65 °C and 5 min at 95 °C) followed by a hard bake (1 h at 300 °C with nitrogen from 190 °C). A titanium/platinum (Ti/Pt, 5 nm/150 nm) adhesive/conductive layer was deposited by sputtering (Alliance Concept AC450). A positive photoresist (AZ1512, 2 μm) was deposited by spin-coating and soft baked at 110 °C for 2 min before direct exposure (Heidelberg Instruments MLA150, 405 nm) and development. Electrode shaping and photoresist removal were performed by chlorine dry etching (Corial 210IL) followed by oxygen plasma (500 W for 30 s). MEAs were encapsulated by spin-coating an adhesion promoter (VM651, 1000 rpm for 10 s + 3000 rpm for 30 s), spin-coating and soft baking a first PI layer (PI2611, 10 μm) followed by a second layer (10 μm) and curing (soft and hard bake). Then, a Si hard mask (1 μm) was deposited by sputtering (Alliance Concept AC450), and the photolithography was repeated. Dry etching (Corial 210IL) of Si and eventually PI and photoresist (respectively, chlorine and oxygen chemistries) allowed the exposure of Pt pads and electrodes. A final Si dry etching removed the remaining hard mask. The MEAs were cut by a laser cutter (Optec MM200-USP) and released by Al anodic dissolution for 15 h. Electrodes were 300 μm in diameter.

Printed Circuit Board: MEAs were connected to printed circuit boards using conducting epoxy (EPO-TEK H20E-FC) placed on the contact pads manually. After, an isolating epoxy (EPO-TEK 302-3M) was used to ensure a stable connection.

Measurements of Thickness and Electrical Resistivity: The thickness was measured with a stylus profilometer (Tencor P-10). The electrical resistivity was measured with a Fluke 73/77 Series III Digital Multimeter.

Atomic Force Microscopy: Surface topography of printed and sputtered platinum electrodes was imaged at room temperature using a Dimension Icon atomic force microscope (Bruker) in PeakForce tapping mode (ScanAsyst Air silicon tip, $f_0 = 70$ kHz, $k = 0.4$ N m⁻¹). Image processing and roughness evaluation were performed using Gwyddion open-source software.

Bending Test: A customized cycling stretcher was used to perform the bending test with a cyclic compressive force (bending radius 9.1 mm). The system included a stepping motor and a dedicated mechanics to bend the array. For each test, the stepping motor frequency was set at 0.5 Hz, which resulted in a cycling speed of 10 mm s⁻¹. The resistance was measured with a digital multimeter (PeakTech 3690).

Electrochemistry: Electrochemical characterizations were performed with a three-electrode (Ag/AgCl reference electrode, Pt counter electrode)

potentiostat (Compact Stat, Ivium) in phosphate buffered saline (pH 7.4) at room temperature. Impedance spectroscopy was performed between 10 Hz and 1 MHz with an AC voltage of 50 mV. CV was obtained by sweeping a cyclic potential at a speed of 50 mV s⁻¹ between -0.6 and 0.8 V. For each electrode, the average response over five cycles was calculated.^[17]

Animal Experiment: Animal experiments were approved by the Département de l'emploi, des affaires sociales et de la santé (DEAS), Direction générale de la santé de la République et Canton de Genève (Switzerland, authorization GE1416). The procedure was previously described.^[18] Female New Zealand White rabbits (>16 weeks, >2 kg) were sedated with an intramuscular injection of xylazine (5 mg kg⁻¹). Anesthesia and analgesia were provided with an intramuscular injection of an anesthetic mix composed of medetomidine (0.5 mg kg⁻¹), ketamine (25 mg kg⁻¹), and buprenorphine (0.03 mg kg⁻¹). Eye drops were placed on the eye to prevent eye drying. The rabbit was placed on a heating pad at 35 °C for the entire procedure. Oxygen was provided with a mask to prevent hypoxia during the anesthesia. The head was shaved and cleaned with 70% ethanol and betadine. Before cortical skin incision, a mix of lidocaine (6 mg kg⁻¹), bupivacaine (2.5 mg kg⁻¹), and epinephrine (0.1 mg kg⁻¹) was injected subcutaneously on the surgical sites. After 5 min, the skin was opened and pulled aside to expose the skull; afterward, the skull was cleaned with cotton swabs. A craniotomy was made to expose the right visual cortex. The electrocorticography array was placed onto the visual cortex. Light flashes (4 ms) at increasing luminance levels (0.05, 0.1, 0.5, 1, 5, 10, and 30 cd s m⁻²) were delivered using a Ganzfeld stimulator (BM6007B9.5, Biomedica Mangoni) positioned close to the contralateral eye. For cortical recordings, the array was connected to a wireless amplifier (W2100-HS32, Multi Channel Systems) and a data acquisition system (W2100, Multi Channel Systems). Data were filtered (0.1–300 Hz) and sampled at 5 kHz; ten sweeps were averaged for each luminance level. Data analysis was performed in MATLAB (MathWorks). The rabbit was euthanized at the end of the recordings, whereas still under anesthesia, with an intravenous injection of pentobarbital (120 mg kg⁻¹).

Cytotoxicity Test In Vitro: The test was performed by an accredited company (Medistri SA) as previously described.^[12] The test was conducted according to the requirement of ISO 10993-5: Biological Evaluation of Medical Devices, in vitro cytotoxicity test; ISO 10993-12: Test article preparation and reference materials; USP 35-NF30 (87): Biological Reactivity test, in vitro; Medistri internal procedure WI 47 and WI 56. Cytotoxicity was assessed on two independent printed platinum-based electrocorticography arrays sterilized with EtO before the test. The test on extraction was performed on each array with a surface area of 6 cm² and a ratio of the product to extraction vehicle of 3 cm² mL⁻¹. The extraction vehicle was Eagle's minimum essential medium supplemented with fetal bovine serum, penicillin–streptomycin, amphotericin B, and L-glutamine. The extraction was performed for 24 h at 37 °C. The extract was added on triplicate culture wells containing a subconfluent L929 cell monolayer (1:1 dilution). The test samples and the control wells were incubated at 37 °C in 5% CO₂ for 24 h. Following incubation, the cell cultures were examined for quantitative cytotoxic evaluation. 50 µL per well of XTT reagent was added to the cells and then incubated at 37 °C in 5% CO₂ for further 3–5 h. An aliquot of 100 µL was then transferred from each well into the corresponding wells of a new plate, and the optical density was measured at 450 nm.

Statistical Analysis and Graphical Representation: Statistical analysis and graphical representation were performed with Prism (GraphPad Software Inc.). The normality test (D'Agostino & Pearson omnibus normality test) was performed in each dataset to justify the use of a parametric or non-parametric test. In each figure, *p*-values are represented as **p* < 0.05, ***p* < 0.01, ****p* < 0.001, and *****p* < 0.0001. Data are reported as the mean ± SD; *n* is used to identify the number of electrodes or measures, and *N* is used to identify the number of arrays.

Acknowledgements

E.B. and L.F. contributed equally to this work. This work has been supported by École Polytechnique Fédérale de Lausanne, Medtronic,

the Wyss Center for Bio and Neuroengineering, and the Swiss National Science Foundation (project number 200021_182670). The authors thank Ivan Furfaro from the EPFL Laboratory for Soft BioElectronic Interface for his help with the bending test.

Conflict of Interest

The authors declare no conflict of interest.

Keywords

electrocorticography, inkjet printing, microelectrode array, platinum, screen printing

Received: November 14, 2019
Published online: January 27, 2020

- [1] M. E. Spira, A. Hai, *Nat. Nanotechnol.* **2013**, *8*, 83.
- [2] D. Reynolds, G. Z. Duray, R. Omar, K. Soejima, P. Neuzil, S. Zhang, C. Narasimhan, C. Steinwender, J. Brugada, M. Lloyd, P. R. Roberts, V. Sagi, J. Hummel, M. G. Bongiorno, R. E. Knops, C. R. Ellis, C. C. Gornick, M. A. Bernabei, V. Laager, K. Stromberg, E. R. Williams, J. H. Hudnall, P. Ritter, M. T. P. S. Group, *N. Engl. J. Med.* **2016**, *374*, 533.
- [3] A. M. Lozano, N. Lipsman, H. Bergman, P. Brown, S. Chabardes, J. W. Chang, K. Matthews, C. C. McIntyre, T. E. Schlaepfer, M. Schulder, Y. Temel, J. Volkmann, J. K. Krauss, *Nat. Rev. Neurol.* **2019**, *15*, 1.
- [4] J. T. Rubinstein, *Lancet* **2002**, *360*, 483.
- [5] D. Ghezzi, *Front. Neurosci.* **2015**, *9*, 290.
- [6] A. T. Chuang, C. E. Margo, P. B. Greenberg, *Br. J. Ophthalmol.* **2014**, *98*, 852.
- [7] Y. Luo, L. da Cruz, *Prog. Retinal Eye Res.* **2016**, *50*, 89.
- [8] M. Schuettler, S. Stiehs, B. V. King, G. J. Suaning, *J. Neural Eng.* **2005**, *2*, S121.
- [9] L. A. Geddes, R. Roeder, *Ann. Biomed. Eng.* **2003**, *31*, 879.
- [10] S. F. Cogan, *Ann. Rev. Biomed. Eng.* **2008**, *10*, 275.
- [11] B. Bachmann, N. Y. Adly, J. Schnitker, A. Yakushenko, P. Rinklin, A. C. Arias, V. Subramanian, M. M. Maharbiz, *Nat. Commun.* **2017**, *2*, 035003.
- [12] L. Ferlauto, M. Leccardi, N. Chenais, S. Gilliéron, P. Vagni, M. Bevilacqua, T. J. Wolfensberger, K. Sivula, D. Ghezzi, *Nat. Commun.* **2018**, *9*, 992.
- [13] S. L. Swisher, M. C. Lin, A. Liao, E. J. Leefflang, Y. Khan, F. J. Pavinatto, K. Mann, A. Naujokas, D. Young, S. Roy, M. R. Harrison, A. C. Arias, V. Subramanian, M. M. Maharbiz, *Nat. Commun.* **2015**, *6*, 6575.
- [14] C. M. Lochner, Y. Khan, A. Pierre, A. C. Arias, *Nat. Commun.* **2014**, *5*, 5745.
- [15] Y. Khan, F. J. Pavinatto, M. C. Lin, A. Liao, S. L. Swisher, K. Mann, V. Subramanian, M. M. Maharbiz, A. C. Arias, *Adv. Funct. Mater.* **2016**, *26*, 1004.
- [16] T. Roberts, J. B. Graaf, C. Nicol, T. Hervé, M. Flocchi, S. Sanaur, *Adv. Healthcare Mater.* **2016**, *5*, 1462.
- [17] L. Ferlauto, A. N. D'Angelo, P. Vagni, M. J. I. A. Leccardi, F. M. Mor, E. A. Cuttaz, M. O. Heuschkel, L. Stoppini, D. Ghezzi, *Front. Neurosci.* **2018**, *12*, 648.
- [18] V. Gaillet, A. Cutrone, F. Artoni, P. Vagni, A. Mega Pratiwi, S. A. Romero, D. Lipucci Di Paola, S. Micera, D. Ghezzi, *Nat. Biomed. Eng.* **2019**, <https://doi.org/10.1038/s41551-019-0446-8>.